⌘ *Author's Choice*

THE JOURNAL OF BIOLOGICAL CHEMISTRY VOL. 285, NO. 34, pp. 26022–26032, August 20, 2010

Recognition of Polyadenosine RNA by the Zinc Finger Domain of Nuclear Poly(A) RNA-binding Protein 2 (Nab2) Is Required for Correct mRNA 3′-End Formation*[S]

Received for publication, May 5, 2010, and in revised form, June 10, 2010 Published, JBC Papers in Press, June 16, 2010, DOI 10.1074/jbc.M110.141127

Seth M. Kelly[‡], Sara W. Leung[‡], Luciano H. Apponi[§], Anna M. Bramley[‡], Elizabeth J. Tran[¶1], Julia A. Chekanova[‖], Susan R. Wente[¶], and Anita H. Corbett[‡2]

From the Departments of [‡]Biochemistry and [§]Pharmacology, Emory University School of Medicine, Atlanta, Georgia 30322, the [¶]Department of Cell and Developmental Biology, Vanderbilt University School of Medicine, Nashville, Tennessee 37232-8240, and the [‖]School of Biological Sciences, University of Missouri, Kansas City, Missouri 64110

Proteins bound to the poly(A) tail of mRNA transcripts, called poly(A)-binding proteins (Pabs), play critical roles in regulating RNA stability, translation, and nuclear export. Like many mRNA-binding proteins that modulate post-transcriptional processing events, assigning specific functions to Pabs is challenging because these processing events are tightly coupled to one another. To investigate the role that a novel class of zinc finger-containing Pabs plays in these coupled processes, we defined the mode of polyadenosine RNA recognition for the conserved *Saccharomyces cerevisiae* Nab2 protein and assessed *in vivo* consequences caused by disruption of RNA binding. The polyadenosine RNA recognition domain of Nab2 consists of three tandem Cys-Cys-Cys-His (CCCH) zinc fingers. Cells expressing mutant Nab2 proteins with decreased binding to polyadenosine RNA show growth defects as well as defects in poly(A) tail length but do not accumulate poly(A) RNA in the nucleus. We also demonstrate genetic interactions between mutant *nab2* alleles and mutant alleles of the mRNA 3′-end processing machinery. Together, these data provide strong evidence that Nab2 binding to RNA is critical for proper control of poly(A) tail length.

Following transcription by RNA polymerase II in the nucleus, mRNA transcripts must be spliced and polyadenylated, exported to the cytoplasm, and perhaps even transported to a distant site of translation (1). Although these steps are often presented as disconnected parts of a tangled web of processing, they are actually tightly coupled to one another and normally function as one integrated machine for producing transcripts ready for translation in the cytoplasm (2). Like any efficient assembly line, early steps in the pathway ready the transcript for subsequent processes. The vast majority of the proteins bound to mRNA transcripts are evolutionarily conserved and have been ascribed multiple functions in mRNA biogenesis. Many of these functions have been inferred from mutant phenotypes (3). However, because of the coupled nature of mRNA processing events (4), the question arises as to whether these proteins actually function in multiple processing/maturation steps or whether a defect in an early step in mRNA biogenesis indirectly causes a problem in steps downstream.

One example of a protein implicated in multiple aspects of RNA biogenesis is the *Saccharomyces cerevisiae* nuclear poly(A)-binding protein 2 (Nab2). Previous studies have demonstrated that Nab2 and its putative orthologue in higher eukaryotes, ZC3H14, bind specifically and with high affinity to polyadenosine RNA *in vitro* (5–7). Importantly, these proteins are members of a novel class of tandem zinc finger (ZnF) proteins that recognize polyadenosine RNA via Cys-Cys-Cys-His (CCCH) zinc fingers (6). In contrast, all other characterized poly(A)-binding proteins (Pabs)[3] bind polyadenosine RNA via at least one well conserved RNA recognition motif (8). Thus, Nab2 and other members of this evolutionarily conserved CCCH zinc finger-containing Pab family must recognize polyadenosine RNA through a fundamentally different mechanism than the RNA recognition motif-containing family of poly(A) RNA-binding proteins. Further characterization of the molecular mechanisms of polyadenosine RNA recognition by CCCH zinc fingers will allow for critical insight into the means by which Pabs post-transcriptionally regulate gene expression.

Nab2 has been implicated in at least two separate but coupled steps in mRNA biogenesis. First, Nab2 modulates poly(A) tail length as *nab2* mutants have extended poly(A) tails *in vivo* (7, 9, 10), and the addition of recombinant Nab2 to *in vitro* polyadenylation assays limits poly(A) tail length (7, 9, 11). Second, Nab2 is implicated in the export of poly(A) RNA from the nucleus (7, 12–14). Some *nab2* mutant cells show poly(A) RNA accumulation within the nucleus, and *nab2* alleles show genetic interactions with genes encoding mRNA export factors, including *YRA1* and *MEX67* (14, 15). Furthermore, Nab2 physically interacts with Mlp1/2 at the inner face of the nuclear pore complex to facilitate export of RNA from the nucleus (16, 17). A logical model based on this information is one in which Nab2 plays a role in polyadenylation, associates with the poly(A) tail of mature mRNA transcripts, interacts with components of the nuclear pore, and subsequently exits the nucleus in complex

⌘ *Author's Choice*—Final version full access.

[S] The on-line version of this article (available at http://www.jbc.org) contains supplemental Figs. 1 and 2.

[1] Present address: Dept. of Biochemistry, Purdue University, West Lafayette, IN 47907-2063.

[2] To whom correspondence should be addressed: Emory University School of Medicine, 1510 Clifton Rd., NE Atlanta, GA 30322-2430. Fax: 404-727-3452; E-mail: acorbe2@emory.edu.

[3] The abbreviations used are: Pab, poly(A)-binding protein; 5-FOA, 5-fluoroorotic acid; nt, nucleotide.

TABLE 1
Strains and plasmids used in this study

Strain/Plasmid	Description	Source
ACY427	Δ*NAB2::HIS* (pAC636) *MATa leu2 ura3*	12
ACY1669	Δ*NAB2::HIS rat8-2* (*dbp5*) *MATa leu2 ura3 trp1*	25
pRS315 (pAC3)	*CEN, LEU2*	43
pAC636	*NAB2, CEN, URA3*	12
pAC717	*NAB2, CEN, LEU2*	12
pAC1945	*PGEX-4T-1* (containing TEV cleavage site instead of thrombin)	44
pAC2027	*Nab2-C262A, CEN, LEU2*	This study
pAC2028	*Nab2-C283A, CEN, LEU2*	This study
pAC2029	*Nab2-C340A, CEN, LEU2*	This study
pAC2030	*Nab2-C371A, CEN, LEU2*	This study
pAC2031	*Nab2-C415A, CEN, LEU2*	This study
pAC2033	*Nab2-C437A, CEN, LEU2*	This study
pAC2035	*Nab2-C458A, CEN, LEU2*	This study
pAC2133	Untagged *NAB2*, pMW172 bacterial expression vector	6
pAC2203	*Nab2-C415A,C437A,C458A, CEN, LEU2*	This study
pAC2222	*Nab2-C415R,C437R,C458R, CEN, LEU2*	This study
pAC2304	*GST-NAB2* zinc fingers 1–7	6
pAC2305	*GST-NAB2* zinc fingers 1–4	This study
pAC2307	*Nab2-C437S, CEN, LEU2*	25
pAC2502	*Nab2-Y428A, CEN, LEU2*	This study
pAC2503	*Nab2-F450A, CEN, LEU2*	This study
pAC2504	*Nab2-F460A, CEN, LEU2*	This study
pAC2505	*Nab2-F471A, CEN, LEU2*	This study
pAC2522	*GST-NAB2* zinc fingers 5–7	This study
pAC2597	*GST-Nab2* zinc fingers 5–7 *F450A, F471A*	This study
pAC2624	*GST-Nab2* zinc fingers 5–7 *Y428A, F450A, F471A*	This study
pAC2672	*Nab2-Y428A, F450A, F471A, CEN, LEU2*	This study
pAC2702	Untagged *Nab2-ΔZnF 5–7*, pMW172 bacterial expression vector	This study
pAC2713	Untagged *Nab2-Y428A*, pMW172 bacterial expression vector	This study
pAC2714	Untagged *Nab2-F450A*, pMW172 bacterial expression vector	This study
pAC2716	Untagged *Nab2-F471A*, pMW172 bacterial expression vector	This study

with the poly(A) tail of mRNA transcripts. However, although it is certainly possible that Nab2 could play roles in both polyadenylation and RNA export from the nucleus, it is also plausible that a defect in one of these coupled processes could indirectly cause the other observed defect. In fact, mutations in many *bona fide* 3′-end processing factors cause poly(A) RNA export defects, whereas defects in select export factors cause longer poly(A) tails (18, 19). As with many RNA-binding proteins that function in highly coupled post-transcriptional RNA processing events (20), a major challenge is to determine the main function of Nab2 in producing mature mRNA transcripts primed for translation in the cytoplasm.

In this study, we precisely defined the high affinity polyadenosine RNA binding domain of Nab2 and then generated *nab2* mutants that would allow us to assess the requirement for Nab2-RNA binding in poly(A) tail length control and poly(A) RNA export from the nucleus. We hypothesized that the essential function of Nab2 requires binding to polyadenosine RNA. In support of this hypothesis, Nab2 zinc fingers 5–7 mediated a high affinity specific interaction between Nab2 and polyadenosine RNA. Furthermore, amino acid substitutions within zinc fingers 5–7 decreased poly(A) RNA binding *in vitro*. Cells that expressed Nab2 RNA-binding mutants showed an increase in poly(A) tail length but no nuclear accumulation of poly(A)RNA suggesting that Nab2 binding to polyadenosine RNA is required for the modulation of poly(A) tail length. In addition, these *nab2* variant alleles genetically interacted with mutant alleles of the mRNA 3′-end processing machinery. These results provide critical insight into the molecular mechanism underlying polyadenosine RNA recognition by CCCH zinc fingers as well as the means by which Pabs can post-transcriptionally regulate gene expression.

EXPERIMENTAL PROCEDURES

Chemicals, Plasmids, and S. cerevisiae Manipulations—Chemicals were obtained from Fisher, Sigma, or United States Biological (Swampscott, MA) unless otherwise noted. DNA manipulations were performed according to standard methods (21), and all media were prepared by standard procedures (22). All *S. cerevisiae* strains and plasmids used in this study are described in Table 1. Plasmids encoding mutant Nab2 proteins were generated by site-directed mutagenesis of a wild-type *NAB2* plasmid (pAC717) using the QuikChange site-directed mutagenesis kit (Stratagene). All plasmids were fully sequenced to ensure that no mutations other than those targeted were introduced during site-directed mutagenesis. The *NAB2* open reading frame was deleted from *S. cerevisiae* strains encoding the 3′-end processing mutants *pap1-1* or *rna15-2* using PCR-based gene disruption essentially as described previously (23).

In Vivo Functional Analysis—The *in vivo* function of each Nab2 mutant was tested using a plasmid shuffle assay (24). *S. cerevisiae* cells deleted for *NAB2* (ACY427) and containing a wild-type *NAB2 URA3* plasmid (pAC636) were transformed with *LEU2* plasmids expressing various Nab2 mutants. Transformants were grown to saturation, and cells were then serially diluted and spotted onto control ura$^-$ leu$^-$ glucose plates or plates containing 5-fluoroorotic acid (5-FOA). Plates were then incubated at 18, 25, 30, or 37 °C for 3–5 days. The toxic uracil analogue, 5-FOA, kills cells that contain a functional uracil biosynthetic pathway (24). Hence, only those cells that lose the *URA3* plasmid encoding wild-type *NAB2* and retain a functional copy of *nab2* on the *LEU2* plasmid will grow on media containing this drug.

For analysis of *rat8-2* (*dbp5*) suppression, a plasmid shuffle assay was performed as described previously (25). Briefly, Δ*NAB2 rat8-2* cells transformed with plasmids expressing wild-type or mutant Nab2 were first grown on selective media containing 5-FOA, then grown on rich media (YPD), and finally grown to saturation, serially diluted, and spotted onto YPD. Plates were then incubated at 16, 18, 25, 30, or 32 °C for 3–5 days.

Protein Expression and Purification—GST-tagged proteins were expressed in *Escherichia coli* and purified essentially as described previously (6). Briefly, plasmids encoding GST, GST-Nab2, GST-Nab2 zinc finger (ZnF) 1–4, or GST-Nab2-ZnF 5–7 were transformed into BL21(DE3) *E. coli* cells. Single colonies were inoculated into 2-ml cultures and grown overnight to saturation. These starter cultures were used to inoculate 50 ml of media. Cultures were grown at 37 °C until they reached an $A_{600\ nm}$ of 0.4–0.6. Protein expression was induced with 200 μM isopropyl β-D-1-thiogalactopyranoside for 5 h at 30 °C. Following protein induction, cells were pelleted and frozen at −80 °C. Frozen cell pellets were resuspended in lysis buffer (20 mM Tris-HCl, pH 8.0, 100 mM NaCl, 5% glycerol, 4 μM 2-mercaptoethanol, 2 μM $ZnCl_2$, 1 mM phenylmethylsulfonyl fluoride) and lysed by sonication. GST-tagged proteins were purified on GST-Sepharose 4B (GE Healthcare) according to the manufacturer's directions. A small amount of purified protein was resolved by SDS-PAGE to determine the purity of the sample. Untagged recombinant proteins were purified essentially as described previously (6). For all assays utilizing untagged proteins, binding assays were performed within 72 h of purification due to an inability to freeze/thaw the Nab2 protein. Thus, experiments always compared results from batches of protein purified on the same day. This approach yielded some modest variation in the absolute number obtained for binding constants (*e.g.* 16 *versus* 29 nM for wild-type Nab2), but these binding constants remained quite consistent within a batch of Nab2 as evidenced by the relatively small standard deviations in the values obtained. Because of this variation, wild-type Nab2 was independently purified, and the binding constant was calculated to provide a relative binding constant within each experimental data set.

RNA Oligonucleotides and Fluorescein Labeling—All RNA oligonucleotides, including Cy3-labeled $r(A)_{25}$, were obtained from Dharmacon (Lafayette, CO) and were deprotected in the supplied deprotection buffer according to the manufacturer's instructions. Deprotected oligonucleotides were evaporated to dryness and stored at −20 °C. For use in anisotropy assays, deprotected RNA oligonucleotides were 3′-end-labeled with fluorescein-5-thiosemicarbazide essentially as described previously (26). Typical labeling efficiencies were ~60–70%.

Fluorescence Anisotropy—In a typical anisotropy experiment, fluorescein-labeled 25-nt poly(A) RNA oligonucleotides were incubated in binding buffer (20 mM Tris-HCl, pH 8.5, 150 mM NaCl, 2% glycerol) with untagged full-length Nab2 or mutant Nab2 protein for ~2 h at room temperature. Typical final concentrations of labeled RNA were 1–2 nM, although protein concentrations varied between 50 pM and 5–10 μM. Binding reactions were then transferred to a 384-well plate, and the apparent fluorescence anisotropy of each sample was determined using a fluorescence plate reader fitted with fluorescein filters and polarizers. Each experiment was performed in triplicate. The percentage of bound fluorescein-labeled oligonucleotide was plotted as a function of protein concentration for each experiment. To determine the apparent dissociation constant (K_d), the data were subsequently fit with Equation 1,

$$f_b = \frac{(K_d + [P]_{tot} + [O]_{tot}) - \sqrt{(K_d + [P]_{tot} + [O]_{tot})^2 - 4\cdot[P]_{tot}\cdot[O]_{tot}}}{2\cdot[O]_{tot}} \quad \text{(Eq. 1)}$$

where [P] and [O], represent the total protein concentration and total oligonucleotide concentration, respectively.

RNA Electrophoretic Mobility Shift Assays—For RNA gel shift assays, a Cy3-labeled 25-nt poly(A) RNA oligonucleotide was incubated in binding buffer (20 mM Tris-HCl, pH 8.5, 50 mM NaCl, 2 μM $ZnCl_2$, 2% glycerol) with GST or GST-tagged proteins as indicated for 20 min at room temperature. Binding reactions were loaded onto a native 5% polyacrylamide gel and electrophoresed in 0.3× TBE for 30–60 min to resolve free Cy3-labeled oligonucleotide from RNA-protein complexes. The position of the Cy3-labeled oligonucleotide within the native gel was determined using a Typhoon phosphorimager (Amersham Biosciences) equipped with a laser capable of exciting Cy3. RNA gel shift competition experiments were performed as described previously (6).

Limited Trypsin Proteolysis and Poly(A)-Sepharose Binding Assays—For partial proteolysis, 3.2 mg of recombinant purified GST-Nab2 was incubated with 20 μg of trypsin for 30 min at room temperature. The entire reaction was then incubated with poly(A)-Sepharose 4B (Sigma); the Sepharose was washed, and bound complexes were eluted. Bound fractions were resolved by SDS-PAGE and either stained with Coomassie Blue or transferred to PVDF membranes for N-terminal sequencing. Edman degradation N-terminal sequencing was performed by the Emory Microchemical Facility to identify the N-terminal eight amino acids of the eluted Nab2 RNA-binding fragments.

Poly(A) Tail Length Determination—Cells expressing wild-type Nab2 or Nab2 mutant proteins were inoculated into YPD media and grown to saturation at 30 °C. Cells were then diluted into 50 ml of YPD and grown at either 30 or 16 °C until they reached $A_{600\ nm}$ of 0.4–0.6. A total of 20 absorbance units of cells was harvested from each culture, and poly(A) tail length was determined as described previously (10, 27). Briefly, total RNA was end-labeled with ^{32}P-pCp and T4 RNA ligase. To digest nonpoly(A) RNA, the ^{32}P-labeled RNA was subsequently digested with RNases A/T1 and then ethanol-precipitated. Resuspended RNA was then resolved by denaturing urea-acrylamide gel electrophoresis and imaged using a phosphorimager. Quantification of poly(A) tail lengths was performed using the ImageJ software package as described previously (28). Densitometry was performed on poly(A) tails comparing the ratio of short ^{32}P-labeled poly(A) tails near the bottom of the gel to longer ^{32}P-labeled poly(A) tails near the top of the gel. For each temperature, this ratio was set to 1.0 for RNA isolated from wild-type cells, and the poly(A) tail ratio from cells expressing mutant Nab2 proteins was compared with wild type to determine whether any significant difference in poly(A) tail length

was observed. A Student's *t* test was performed to determine significant differences in poly(A) tail length ratios.

Fluorescence in Situ Hybridization (FISH)—Cells expressing wild-type Nab2 or Nab2 mutant proteins were initially grown in 2-ml cultures to saturation at 30 °C. These starter cultures were then used to inoculate 10-ml cultures that were grown overnight (~12–16 h) at 30 °C. Cultures were then split into two 5-ml cultures and grown at either 30 or 16 °C. Cells were then fixed by the addition of 700 μl of 37% formaldehyde and incubated at 30 or 16 °C for 90 min, and FISH using an oligo(dT) probe to detect poly(A) RNA was performed as described previously (29). Cells were also stained with 4′,6-diamidino-2-phenylindole (DAPI) to visualize DNA within the nucleus.

RESULTS

To define the RNA-binding module of Nab2, we first exploited a previously described genetic interaction between *NAB2* and *DBP5*, which encodes the nuclear pore associated mRNA-protein complex remodeler (30–32) (also called Rat8 (33)). Importantly, an amino acid substitution in the RNA binding domain of Nab2, Nab2-C437S, which decreases the affinity of Nab2 for polyadenosine RNA 4-fold (6), suppresses the growth defect and poly(A) RNA accumulation of a Dbp5 mutant *rat8-2* (*dbp5*) (25). These data suggest that if the RNA binding affinity of a Dbp5 substrate, such as Nab2, is decreased, as in Nab2-C437S, a partially functional mutant Dbp5 protein may retain sufficient remodeling activity to remove the weakly bound Nab2-C437S protein from the mRNA transcript. This model implies that other Nab2 mutants that weaken the interaction of Nab2 with polyadenosine RNA may also suppress the temperature-sensitive phenotype of the *rat8-2* (*dbp5*) mutant. Hence, this genetic assay was employed as a simple approach to identify putative residues that are critical for Nab2 binding to RNA.

To determine which of the seven zinc fingers in Nab2 are important for RNA binding, we generated point mutants that result in cysteine to alanine amino acid changes in the first cysteine of each of the seven zinc fingers (Fig. 1*A*), and we tested whether these mutants could suppress the temperature-sensitive growth phenotype of the *rat8-2* (*dbp5*) mutant at 32 °C. As shown in Fig. 1*B*, individual cysteine to alanine substitutions within each of the first cysteines of Nab2 zinc fingers 1–4 did not suppress the temperature-sensitive phenotype of the *rat8-2* (*dbp5*) mutant. In contrast, individual cysteine to alanine substitutions in each of the first cysteines of zinc fingers 5–7 did suppress the temperature-sensitive growth phenotype of the *rat8-2* (*dbp5*) mutant. This genetic result suggests that only the last three zinc fingers of Nab2 may be necessary for polyadenosine RNA binding.

We also used a biochemical approach to define the domain of Nab2 that binds to polyadenosine RNA. The genetic suppression assay (Fig. 1*B*) implicates zinc fingers 5–7 in binding to polyadenosine RNA. To test this prediction, we expressed and purified recombinant Nab2 protein fragments containing zinc fingers 1–7 (amino acids 262–473), zinc fingers 1–4 (amino acids 262–387), or zinc fingers 5–7 (amino acids 403–477) as GST fusion proteins. To assess RNA binding for each of these domains, RNA gel shift assays were used to examine binding of

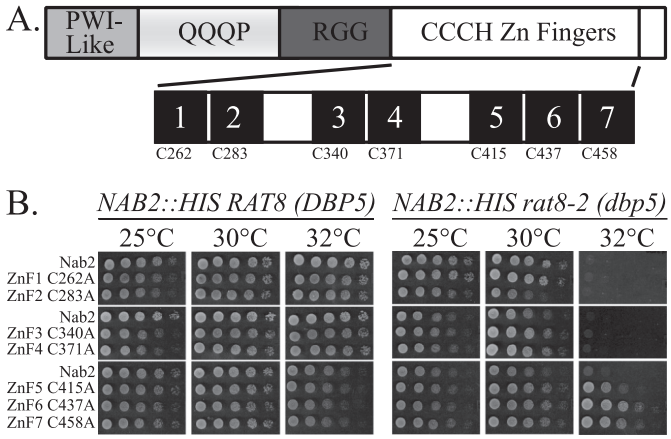

FIGURE 1. **Cysteine to alanine substitutions in Nab2 zinc fingers 5–7 result in mutants that suppress the temperature-sensitive phenotype of *rat8-2* (*dbp5*) cells.** *A,* schematic depicting the domains of *S. cerevisiae* Nab2. The C-terminal CCCH zinc finger domain contains seven tandem zinc fingers (*black boxes*). The position of the first cysteine of each zinc finger is indicated *below* the corresponding zinc finger. *B, S. cerevisiae* plasmid shuffle assay analyzing the suppression of the temperature-sensitive growth phenotype of *rat8-2* (*dbp5*) cells by the indicated Nab2 mutants. Δ*NAB2* cells harboring a *URA3* plasmid encoding wild-type Nab2 and expressing either wild-type Dbp5 (*left panel*) or the mutant Rat8–2 (dbp5) (*right panel*) were transformed with *LEU2* plasmids containing either wild-type Nab2 or Nab2 with the denoted individual changes resulting in cysteine to alanine substitutions in zinc fingers 1–7 (ZnF 1–7). Transformants were streaked to media containing 5-FOA to select against cells retaining the *URA3* wild-type *NAB2* plasmid. Cells were then inoculated into YPD liquid, grown to saturation at 25 °C, serially diluted, and spotted onto YPD plates. Plates were incubated at 25, 30, or 32 °C.

each protein to a Cy3-labeled poly(A)$_{25}$ RNA oligonucleotide (Cy3-r(A)$_{25}$). As shown in Fig. 2*A*, neither GST alone nor GST-zinc fingers (ZnF) 1–4 bound the Cy3-labeled poly(rA)$_{25}$ oligonucleotide, but GST-ZnF 1–7 and GST-ZnF 5–7 both bound to Cy3-r(A)$_{25}$. Binding of Nab2 zinc fingers 5–7 was specific for stretches of polyadenosine RNA because only unlabeled poly(A) RNA oligonucleotide (r(A)$_{25}$) and not a randomized 25-nt RNA oligonucleotide (r(N)$_{25}$) competed for binding (Fig. 2*B*).

To determine whether ZnF 5–7 are necessary for high affinity binding of Nab2 to polyadenosine RNA, we used fluorescence anisotropy to quantitatively measure binding of full-length Nab2 or Nab2 ΔZnF 5–7 (lacking residues 403–525) to fluorescein-labeled poly(A)$_{25}$ RNA oligonucleotides. Both full-length Nab2 and Nab2 ΔZnF 5–7 were expressed and purified from bacteria as untagged recombinant proteins. As shown in Fig. 2*C*, wild-type Nab2 bound the fluorescein-labeled poly(A)$_{25}$ RNA oligonucleotides with an apparent K_d of 29.7 ± 2 nM, which is consistent with previous studies (6, 7). Interestingly, Nab2 ΔZnF 5–7 bound the poly(A)$_{25}$ RNA oligonucleotide significantly more weakly (~50-fold), with an apparent K_d of 1.7 ± 0.1 μM. This finding confirms that ZnF 5–7 constitute the primary high affinity binding site for polyadenosine RNA. The binding affinity of the Nab2 ZnF 5–7 domain alone for fluorescein-labeled poly(A)$_{25}$ RNA oligonucleotide was not investigated due to the small molecular mass of the Nab2 ZnF 5–7 domain (~9 kDa). We estimated that the difference in anisotropy between the bound and unbound state would be extremely small and therefore would result in a grossly inaccurate calculation of the binding affinity for this interaction.

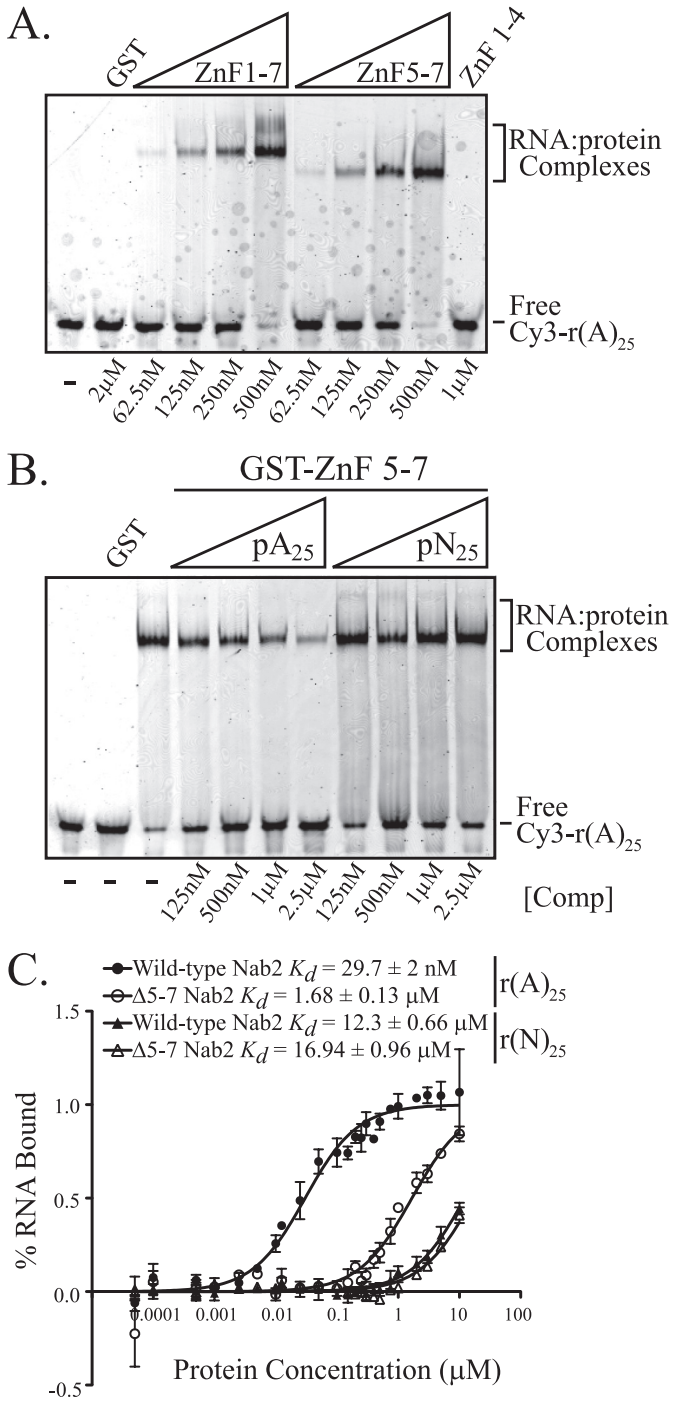

FIGURE 2. **Nab2 zinc fingers 5–7 are necessary and sufficient to mediate specific binding to polyadenosine RNA.** *A*, GST (2 μM), GST ZnF 1–7 (62.5 nM-500 nM), GST ZnF 5–7 (62.5 nM-500 nM), or GST ZnF 1–4 (1 μM) as indicated below the gel was incubated with ~125 nM Cy3-labeled poly(A) RNA oligonucleotide for 20 min at room temperature. RNA-protein complexes were resolved from free probe by nondenaturing electrophoresis in a 5% polyacrylamide gel. The position of the free probe is evident (free Cy3-r$(A)_{25}$) in the control lane with no protein added (−). *B*, binding specificity of GST ZnF 5–7 was investigated by incubating 250 nM GST ZnF 5–7 with 115 nM Cy3-r$(A)_{25}$ in the presence of 125 nM to 2.5 μM unlabeled 25-nt poly(A) RNA oligonucleotide (pA_{25}) competitor or 125 nM to 2.5 μM unlabeled 25-nt randomized RNA oligonucleotide (pN_{25}) competitor. RNA-protein complexes were resolved from free probe by nondenaturing electrophoresis in a 5% polyacrylamide gel. The position of free Cy3-pA (Cy3-r$(A)_{25}$) is indicated. Competitor concentration ([*Comp*]) and those samples containing no competitor (−) are indicated. As a control, no binding to Cy3-r$(A)_{25}$ is observed with 2 μM GST. *C*, binding of increasing concentrations of untagged full-length Nab2 or untagged Nab2 ΔZnF 5–7 to 1 nM fluorescein-labeled poly(A) RNA oligonucleotide (r$(A)_{25}$) or 2 nM poly(N) RNA oligonucleotide (r$(N)_{25}$) was analyzed by fluorescence anisotropy as described under "Experimental Procedures." The % bound RNA is plotted as a function of Nab2 protein concentration. Each binding experiment was performed in triplicate. K_d values and associated standard deviations in the data are indicated.

The relatively weak binding of Nab2 ΔZnF 5–7 to poly$(A)_{25}$ suggests that Nab2 might contain a sequence nonspecific RNA binding domain outside of ZnF 5–7. To test this idea, binding of both Nab2 and Nab2 ΔZnF 5–7 to random RNA sequences (fluorescein-labeled poly$(N)_{25}$ RNA) was analyzed by fluorescence anisotropy. As shown in Fig. 2*C*, both full-length Nab2 (K_d = 12.3 μM) and Nab2 ΔZnF 5–7 (K_d = 16.9 μM) bound very weakly to fluorescein-labeled poly$(N)_{25}$.

As a complementary and unbiased biochemical approach to define an independently folding domain within Nab2 that might bind polyadenosine RNA, GST-tagged recombinant Nab2 was expressed and purified from *E. coli* and subjected to partial trypsin proteolysis. Trypsinized Nab2 fragments were then incubated with poly(A)-Sepharose, and bound fragments were eluted, separated by SDS-PAGE, and transferred to a PVDF membrane. A prominent band of ~10 kDa was then N-terminally sequenced to define the Nab2 poly(A) binding domain (supplemental Fig. 1). This analysis led to the identification of three nested protein fragments with N termini immediately upstream of zinc finger 5. Based upon the mass of these protein fragments, each was predicted to contain zinc fingers 5–7. These data suggest that the Nab2 domain containing CCCH zinc fingers 5–7 mediates specific high affinity binding to poly(A) RNA *in vitro*.

We hypothesized that amino acid substitutions within zinc fingers 5–7 that are predicted to disrupt the structural integrity of the CCCH zinc fingers would impair the function of the essential Nab2 protein and have consequences *in vivo*. To test this hypothesis and examine the impact of these amino acid substitutions on Nab2 function *in vivo*, a plasmid shuffle assay was performed (24). Cells deleted for the essential *NAB2* gene and complemented by a wild-type *NAB2* maintenance plasmid were transformed with plasmids encoding a control wild-type Nab2 or various Nab2 mutant proteins containing individual cysteine to alanine (Cys → Ala) or cysteine to arginine (Cys → Arg) amino acid changes in the first cysteine of zinc fingers 5–7. These cells were then serially diluted and spotted onto control plates and plates containing 5-fluoroorotic acid (5-FOA) to select against the wild-type maintenance plasmid and reveal any phenotype of cells with only the Nab2 mutant proteins. Single Cys → Ala or Cys → Arg substitutions at the first cysteine of individual CCCH zinc fingers 1–7 did not impair Nab2 function as the cells expressing these mutants as the sole copy of Nab2 grew in a manner indistinguishable from wild-type cells (Figs. 1*B* and 3). As a control, cells that express a Nab2 variant lacking the N-terminal 97 amino acids of Nab2 (ΔN-Nab2) and display a severe growth defect (12) were also serially diluted and spotted on the same plates. To assess the consequence of impairing the function of multiple zinc fingers, we constructed plasmids encoding combinations of Cys → Ala or Cys → Arg amino acid substitutions at the first cysteine of zinc fingers 5–7 (Nab2-C_{5-7}→A). Cells expressing *nab2* alleles con-

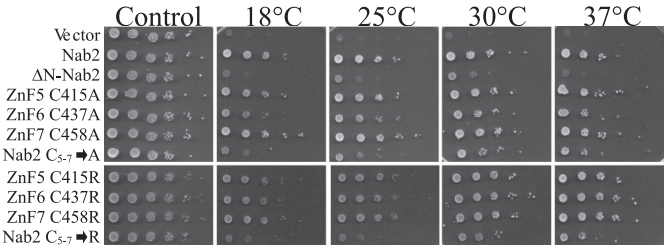

FIGURE 3. **Combinatorial cysteine substitutions in Nab2 zinc fingers 5–7 impair Nab2 function.** Δ*NAB2* cells harboring a *URA3* plasmid encoding wild-type Nab2 were transformed with *LEU2* plasmids encoding either wild-type Nab2, ΔN-Nab2 (missing amino acids 3–97), or Nab2 mutant proteins that contain the denoted individual or combinatorial cysteine to alanine or cysteine to arginine substitution(s) in ZnF 5–7. $C_{5-7}\rightarrow$A or $C_{5-7}\rightarrow$R indicates that the first cysteines of ZnF 5 (Cys-415), 6 (Cys-437), and 7 (Cys-458) were all changed to alanine or arginine, respectively. Transformants were inoculated into liquid media, grown to saturation at 30 °C, and serially diluted. Dilutions were then spotted onto either control media lacking both uracil and leucine or media containing 5-FOA to eliminate the wild-type Nab2 maintenance plasmid. The control plate was incubated at 30 °C for 2 days, although plates containing 5-FOA were incubated at the indicated temperatures for 3–5 days.

taining these triple Cys → Ala or Cys → Arg amino acid substitutions showed greatly diminished viability at 18 °C, suggesting that a combination of these amino acid changes impacts the essential function of the Nab2 protein. This loss of Nab2 function is not due to changes in the level of the Nab2 protein as immunoblotting reveals that all Nab2 proteins were expressed at approximately equal levels in exponentially growing yeast cells at either 30 or 18 °C (data not shown).

To test whether the combination of cysteine to alanine substitutions within zinc fingers 5–7 disrupts RNA binding *in vitro*, we expressed and purified recombinant wild-type GST-ZnF 1–7; GST-ZnF 1–7 C415A,C437A,C458A (GST-ZnF 1–7 $C_{5-7}\rightarrow$A); wild-type GST-ZnF 5–7; and GST-ZnF 5–7 C415A, C437A,C458A (GST-ZnF 5–7 $C_{5-7}\rightarrow$A) and analyzed binding of each of these proteins to a Cy3-labeled poly(A) RNA oligonucleotide in RNA gel shifts assays. As diagrammed in Fig. 4*A*, both GST-ZnF 1–7 $C_{5-7}\rightarrow$A and GST-ZnF 5–7 $C_{5-7}\rightarrow$A contain cysteine to alanine amino acid changes in the first cysteines of zinc fingers 5 (C415A), 6 (C437A), and 7 (C458A).

As shown previously (Fig. 2), wild-type GST ZnF 5–7 bound Cy3-labeled poly(A) RNA oligonucleotide; however, GST-ZnF 5–7 $C_{5-7}\rightarrow$A showed no detectable binding to Cy3-r$(A)_{25}$ (Fig. 4*B*). To determine whether Nab2 zinc fingers 5–7 were necessary for polyadenosine RNA binding, we changed the first cysteine of zinc fingers 5–7 to alanine in the context of the full zinc finger domain (ZnF 1–7). As expected (Fig. 2) (6), wild-type GST-ZnF 1–7 bound the Cy3-labeled polyadenosine oligonucleotide; however, GST-ZnF 1–7 $C_{5-7}\rightarrow$A did not bind Cy3-r$(A)_{25}$ (Fig. 4*C*). These *in vitro* binding data strongly support our conclusion that the Nab2 domain containing zinc fingers 5–7 mediates high affinity binding to poly(A) RNA.

Because of the structural role cysteines and histidines are likely to play in the three-dimensional folding of any CCCH zinc finger (34, 35), cysteine to alanine substitutions in the zinc finger domain of Nab2 are likely to abolish binding to polyadenosine RNA by altering the structure of the zinc finger domain. The cysteines and histidines of most zinc fingers, however, usually make no direct contact with nucleic acids and instead act as structural scaffolds (34). These scaffolds allow other residues,

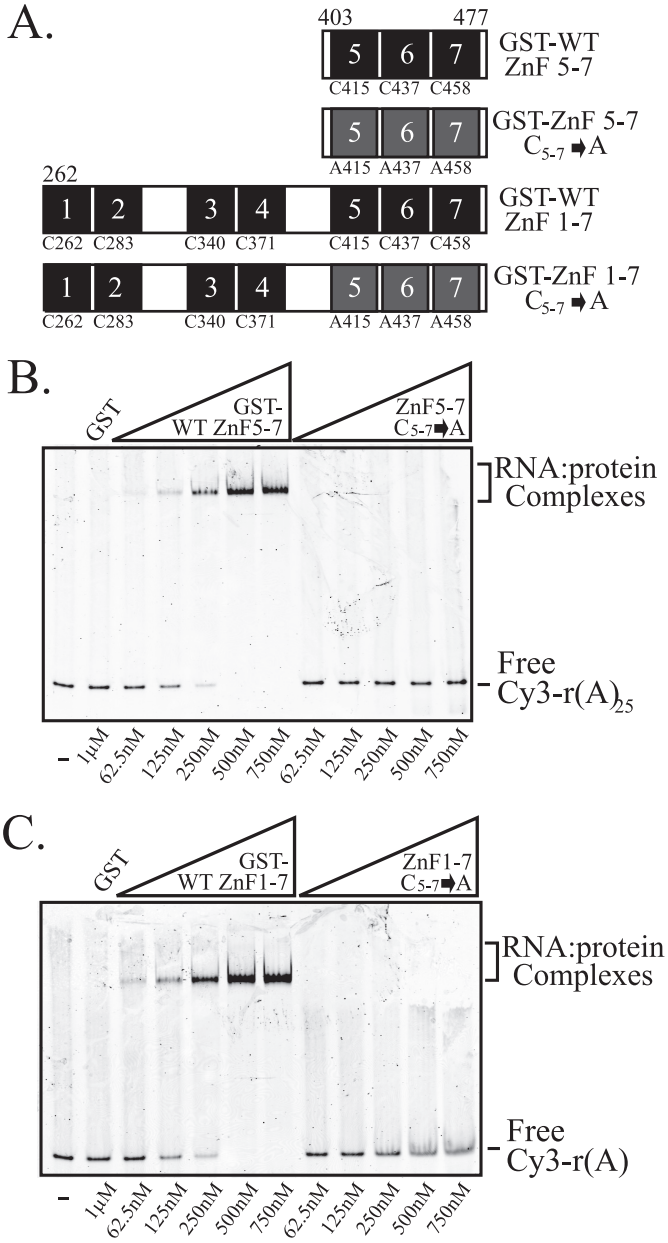

FIGURE 4. **Combinatorial cysteine to alanine substitutions in Nab2 zinc fingers 5–7 cause defects in polyadenosine RNA binding.** *A,* schematic of proteins used in RNA gel shift assays. GST ZnF 5–7 proteins contain Nab2 residues 403–477, and GST ZnF 1–7 proteins contain Nab2 residues 262–477. GST ZnF 5–7 $C_{5-7}\rightarrow$A and GST ZnF 1–7 $C_{5-7}\rightarrow$A contain cysteine to alanine substitutions in the first cysteines of zinc fingers 5 (C415A), 6 (C437A), and 7 (C458A). *B,* combinatorial cysteine to alanine substitutions in ZnF 5–7 abolish RNA binding. GST (1 μM), GST ZnF 5–7 (62.5-500 nM), and GST ZnF 5–7 $C_{5-7}\rightarrow$A (62.5-500 nM) were incubated with ~125 nM Cy3-labeled poly(A) RNA oligonucleotide. RNA-protein complexes were resolved from free probe by electrophoresis in a 5% nondenaturing polyacrylamide gel. The position of the free probe (Cy3-r$(A)_{25}$) is evident in the control lane with no protein added (−). *C,* combinatorial cysteine to alanine substitutions in ZnF 5–7 abolish RNA binding in the context of the entire Nab2 zinc finger domain. GST (1 μM), GST ZnF 1–7 (62.5-500 nM), and GST ZnF 1–7 $C_{5-7}\rightarrow$A (62.5-500 nM) were incubated with ~125 nM Cy3-labeled poly(A) RNA oligonucleotide. RNA-protein complexes were resolved from free probe (Cy3-pA) by electrophoresis in a 5% nondenaturing polyacrylamide gel. Competitor concentration ([*Comp*]) and those samples containing no competitor (−) are indicated. As a control, no binding to Cy3-r$(A)_{25}$ was observed with 1 μM GST.

interspersed between the cysteines and histidines, to be positioned in a way such that they specifically interact with nucleic acids (34). To identify the intervening residues within zinc fin-

gers 5–7 of Nab2 that might specifically interact with polyadenosine RNA, we analyzed an alignment of zinc fingers from Nab2 orthologues with the prediction that residues playing crucial roles in polyadenosine RNA recognition would be conserved between species. Based on this analysis, we identified several aromatic residues (Tyr-428, Phe-450, and Phe-471) within zinc fingers 5–7 of Nab2 that are conserved in higher eukaryotic Nab2 orthologues and that have the potential to form base stacking interactions with polyadenosine RNA (*underlined* residues in Fig. 5*A*).

To analyze the contributions of these aromatic residues (Tyr-428, Phe-450, and Phe-471) within zinc fingers 5–7 to Nab2 function, we constructed alleles that result in these three residues being changed to alanine, either individually or in combination, and we assessed whether these mutants could suppress the temperature-sensitive growth defect of the *rat8-2* (*dbp5*) mutant. We also examined Phe-460, an aromatic residue in zinc finger seven that is located between the first and second cysteine residues, by changing the phenylalanine to alanine. Expression of either Nab2-F450A or Nab2-F471A suppressed the temperature-sensitive growth phenotype of *rat8-2* (*dbp5*) cells (Fig. 5*B*). Expression of Nab2-Y428A or Nab2-F460A did not suppress the temperature-sensitive growth phenotype of *rat8-2* (*dbp5*) cells, suggesting that specific aromatic residues may make direct contacts with polyadenosine RNA, although other aromatic residues are not required for polyadenosine RNA recognition. We also tested the function of each of these mutant proteins by determining whether they could replace Nab2 *in vivo*. As shown in Fig. 5*C*, yeast cells expressing the individual aromatic mutants Y428A, F450A, F460A, or F471A as the only copy of the essential *NAB2* gene grew in a manner indistinguishable from cells expressing a wild-type *NAB2* allele. However, cells expressing an allele of *nab2* that encodes a triple (Y428A,F450A,F471A) mutant showed a significant cold-sensitive growth defect. Similar results were observed when yeast cell growth in liquid culture was analyzed over time by measuring absorbance at 600 nm using a plate reader (supplemental Fig. 2).

Finally, to assess more precisely the contributions of these aromatic residues to polyadenosine RNA recognition, untagged full-length wild-type Nab2 as well as untagged full-length Nab2-Y428A, Nab2-F450A, or Nab2-F471A recombinant protein was purified from *E. coli*, and binding of each of these proteins to fluorescein-labeled $r(A)_{25}$ was analyzed using fluorescence anisotropy (Fig. 5*D*). As expected, wild-type full-length Nab2 bound $r(A)_{25}$-fluorescein with a K_d of 16.3 ± 2 nM). The Y428A and F471A amino acid changes decreased the affinity of full-length Nab2 for poly(A) RNA to 71.8 ± 8 or 56.3 ± 5 nM, respectively. Interestingly, Nab2-F450A had an even greater reduction in binding affinity for $r(A)_{25}$-fluorescein (K_d = 172 ± 12 nM). Taken together, these data suggest that poly(A) RNA recognition by Nab2 requires specific aromatic amino acids within zinc fingers 5–7.

Nab2 has been implicated in the control of poly(A) tail length as well as poly(A) RNA export from the nucleus (7, 12, 17). Presumably, the growth defects seen in Nab2 RNA-binding mutants can be attributed to defects in one or both of these essential functions. To examine the direct requirement for Nab2 binding to RNA in each of these processes, we tested whether cells expressing Nab2 variants defective for RNA binding show changes in poly(A) tail length, poly(A) RNA export from the nucleus, or both processes.

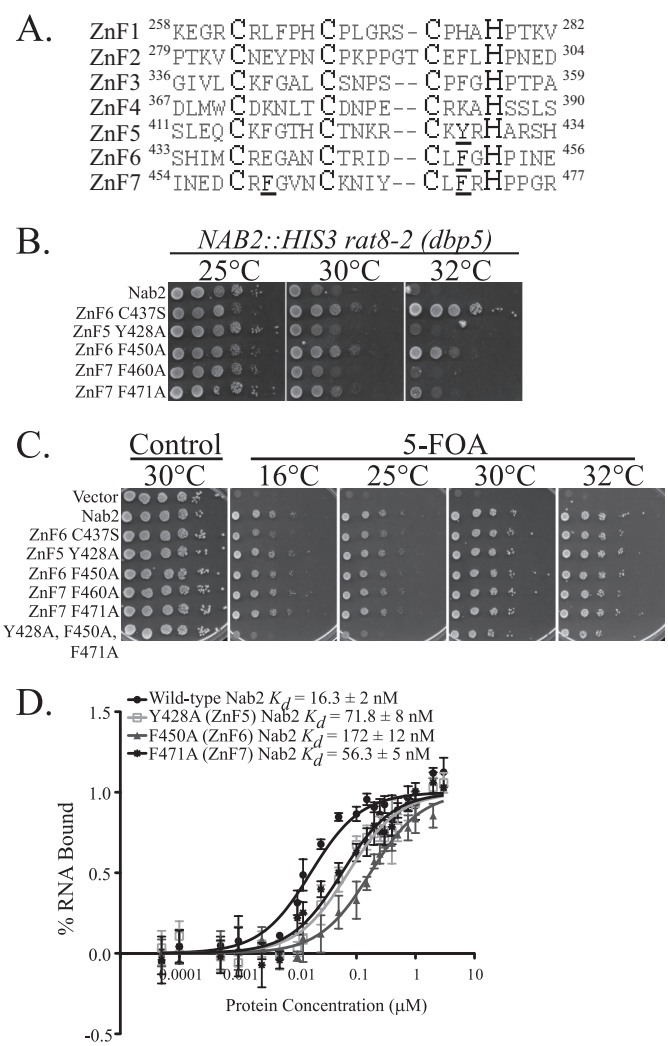

FIGURE 5. **Evolutionarily conserved aromatic residues in Nab2 zinc fingers 5–7 are critical for Nab2 function and binding to polyadenosine RNA.** *A,* alignment of the seven Nab2 CCCH zinc fingers. Numbers corresponding to the first and last amino acid are shown surrounding each zinc finger. Cysteines and histidines are larger and shown in *boldface*, and conserved aromatic residues (Tyr-428, Phe-450, Phe-460, and Phe-471) are shown in *boldface* and *underlined*. *B, S. cerevisiae* plasmid shuffle assay analyzing the suppression of the temperature-sensitive growth phenotype of *rat8-2* (*dbp5*) cells by the indicated Nab2 aromatic mutants. Δ*NAB2* cells complemented by a plasmid encoding wild-type Nab2 and expressing the mutant Rat8-2 (dbp5) were transformed with plasmids encoding either wild-type Nab2, Nab2-C437S, or Nab2 mutant proteins that contain the denoted individual tyrosine or phenylalanine to alanine substitution in zinc fingers 5–7. Transformants were streaked to media containing 5-FOA to select against cells retaining the wild-type maintenance plasmid. Cells were then inoculated into YPD liquid, grown to saturation at 25 °C, serially diluted, and spotted onto YPD plates. *C,* plasmid shuffle assay analyzing the function of individual or combinatorial aromatic Nab2 mutants. Δ*NAB2* cells harboring a *URA3* plasmid encoding wild-type Nab2 were transformed with *LEU2* plasmids encoding wild-type Nab2, Nab2-C437S, or Nab2 proteins that contain the denoted individual or combinatorial cysteine to alanine or cysteine to arginine substitution(s) in ZnF 5–7. Cells were spotted onto either control media lacking both uracil and leucine or media containing 5-FOA to eliminate the wild-type Nab2 maintenance plasmid. *D,* binding of increasing concentrations of untagged full-length Nab2 or untagged Nab2 aromatic mutant proteins (Y428A, F450A, or F471A) to 1 nM fluorescein-labeled poly(A) RNA oligonucleotide was analyzed by fluorescence anisotropy as described under "Experimental Procedures." The % bound RNA is plotted as a function of total protein concentration. Binding was performed in triplicate. K_d values and standard deviations in the data are indicated.

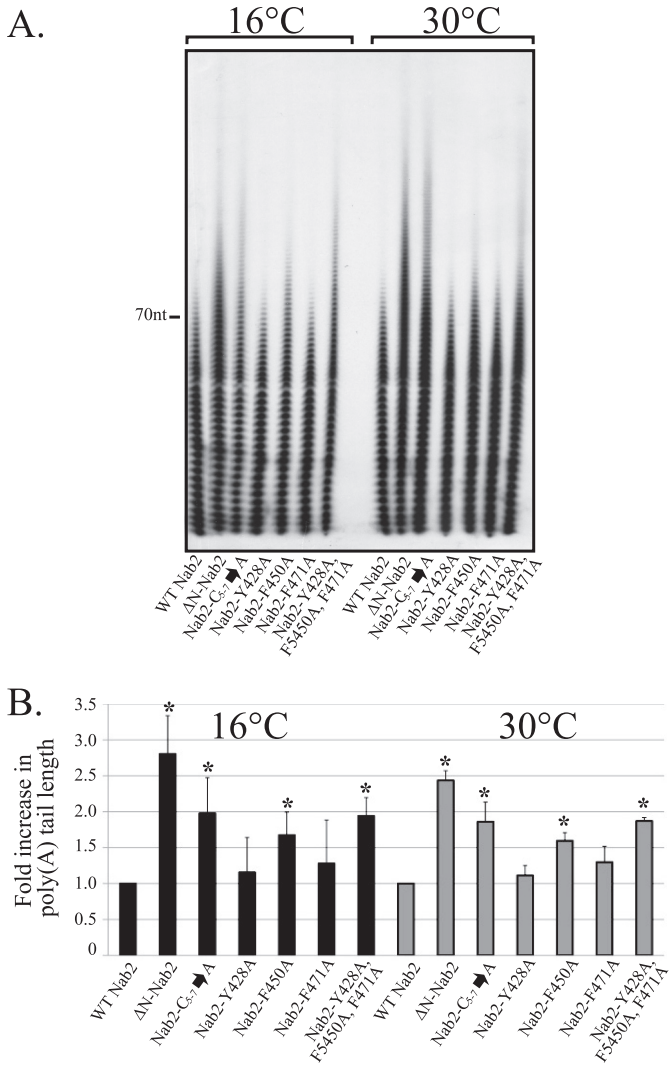

FIGURE 6. **Cells that express Nab2 mutants defective for RNA binding show longer poly(A) tails.** *A,* total RNA was isolated from yeast cells grown at 16 or 30 °C expressing wild-type Nab2, ΔN-Nab2, Nab2-C_{5-7}→A, Nab2-Y428A, Nab2-F450A, Nab2-F471A, or Nab2-Y428A,F450A,F471A and end-labeled with ^{32}P-pCp and T4 RNA ligase. RNA was then digested with RNase A and RNase T1 to digest nonpoly(A) RNA tracts. Resulting stretches of poly(A) RNA were then resolved by denaturing urea-polyacrylamide gel electrophoresis and visualized by autoradiography. The position of the 70 nucleotide (*nt*) typical poly(A) tail length marker is indicated to the *left*. *B,* quantification of poly(A) tail length. The ratio of longer poly(A) tails (greater than ~90–100 nts) to shorter poly(A) tails (near the gel origin) was set to 1.0 for wild-type (*WT*) cells at both 16 °C (*black bars*) and 30 °C (*gray bars*). Standard deviations in the data are indicated ($n = 3$). Poly(A) tails from cells expressing mutant copies of Nab2 that were significantly longer, as determined by a *t* test, than wild-type poly(A) tails at a given temperature are denoted by *asterisks* ($p < 0.05$).

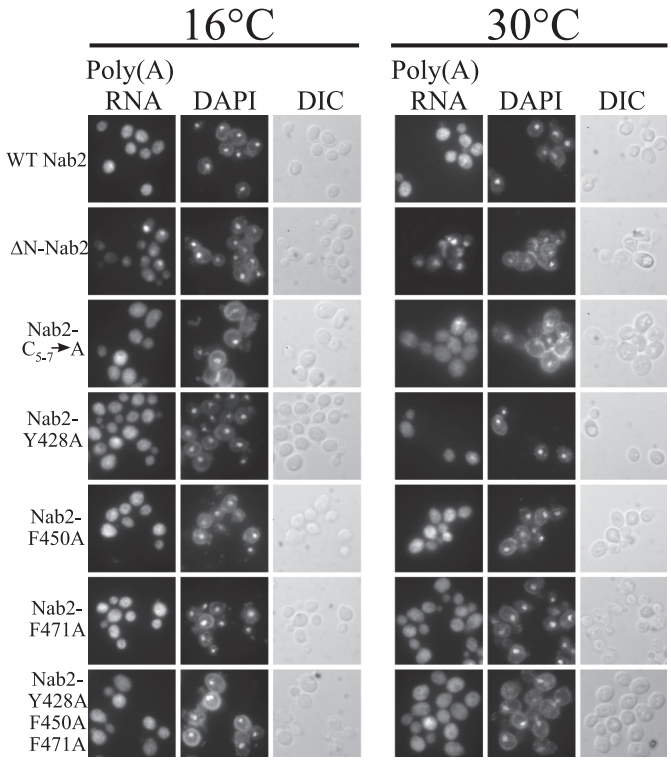

FIGURE 7. **Cysteine to alanine amino acid substitutions within the Nab2 polyadenosine RNA binding domain do not cause accumulation of poly(A) RNA in the nucleus.** FISH using an oligo(dT) probe to detect poly(A) RNA was performed on yeast cells expressing wild-type Nab2, ΔN-Nab2, Nab2-C_{5-7}→A, Nab2-Y428A, Nab2-F450A, Nab2-F471A, or Nab2-Y428A, F450A,F471A. Corresponding DAPI and differential interfering contrast (*DIC*) images are shown.

RNA isolated from cells depleted for Nab2 or cells containing mutant alleles of *NAB2* display longer tracts of poly(A) than wild-type cells (7, 10). We therefore postulated that the growth defect seen in cells expressing Nab2-C415A,C437A,C458A (Nab2-C_{5-7}→A) or Nab2-Y428A, F450A, F471A could be due to deregulation of polyadenylation. To test this hypothesis, we analyzed poly(A) tail length in yeast cells expressing wild-type Nab2 or various Nab2 mutant proteins (Fig. 6). As expected, cells expressing wild-type Nab2 showed normal poly(A) tail length, whereas those expressing ΔN-Nab2 showed extended poly(A) tails at both 30 and 16 °C (7, 10). Yeast cells expressing Nab2-C_{5-7}→A also showed longer poly(A) tails at both temperatures. Interestingly, cells expressing Nab2-F450A showed significantly longer poly(A) tails at both 30 and 16 °C, whereas the Nab2-Y428A and Nab2-F471A mutants caused no significant increase in poly(A) tail length (Fig. 6, *A* and *B*). Extended poly(A) tails were also observed in RNA isolated from cells expressing the triple Nab2-Y428A,F450A,F471A mutant. Together, these results provide a direct correlation between polyadenosine RNA binding affinity and poly(A) tail length and suggest that Nab2 RNA binding is critical for proper control of poly(A) tail length.

To examine whether changes within the CCCH zinc finger binding domain of Nab2 cause defects in poly(A) RNA export, we used FISH to localize poly(A) RNA transcripts in cells expressing Nab2, ΔN-Nab2 (which displays a poly(A) RNA export defect (12) and serves as a positive control in this experiment), and other Nab2 zinc finger mutants (Fig. 7). As expected, cells expressing wild-type Nab2 showed no accumulation of poly(A) RNA in the nucleus, although cells expressing ΔN-Nab2 displayed a significant accumulation of poly(A) RNA in the nucleus at both 30 and 16 °C (Fig. 7). Cells expressing any of the zinc finger mutants, including Nab2-C_{5-7}→A and Nab2-Y428A,F450A,F471A, showed no detectable nuclear accumulation of poly(A) RNA at 30 or 16 °C. This result suggests that the growth defect seen in cells expressing Nab2-C_{5-7}→A or Nab2-Y428A,F450A,F471A is not due to a primary defect in the export of poly(A) RNA from the nucleus.

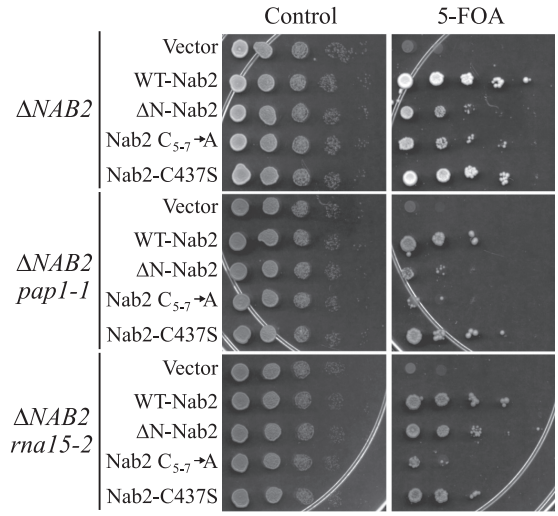

FIGURE 8. **Nab2 genetically interacts with mRNA 3′-end processing components.** Δ*NAB2* (*top row*), Δ*NAB2 pap1-1* (*middle row*), or Δ*NAB2 rna15-2* (*bottom row*) cells harboring a *URA3* plasmid encoding wild-type *NAB2* were transformed with *LEU2* plasmids encoding either wild-type Nab2, ΔN-Nab2, Nab2-C_{5-7}→A, or Nab2-C437S. Cells were spotted onto either control media lacking both uracil and leucine (*Control*) or media containing 5-FOA to eliminate the wild-type Nab2 maintenance plasmid and incubated at 25 °C for 3–5 days.

Results of our analysis provide evidence that Nab2 plays a critical role in mRNA 3′-end formation, suggesting that mutant alleles of *nab2* might show genetic interactions with components of the mRNA 3′-end processing machinery responsible for cleavage and polyadenylation. To test for an interaction with the mRNA 3′-end processing machinery, the *NAB2* gene was deleted in yeast cells expressing either a mutant allele of the poly(A) polymerase, *pap1-1* (36), or a mutant allele of a component of the cleavage machinery, *rna15-2* (27). Cells deleted for the essential *NAB2* gene were complemented by a wild-type *NAB2* maintenance plasmid and transformed with plasmids encoding either wild-type Nab2, ΔN-Nab2, Nab2-C_{5-7}→A, or Nab2-C437S. Cells were then serially diluted and spotted onto either control plates or plates containing 5-FOA to select against the wild-type *NAB2* maintenance plasmid. As shown in Fig. 8, cells expressing Nab2-C_{5-7}→A in combination with either Pap1-1 or Rna15-2 showed a severe growth defect at 25 °C, further supporting the hypothesis that Nab2 RNA binding plays a critical role in 3′-end formation. In addition, Δ*N-Nab2* showed little or no genetic interaction with *pap1-1* or *rna15-2*, suggesting that any genetic interaction between *NAB2* and *RNA15* may be allele-specific and perhaps directly related to the decreased polyadenosine RNA binding affinity of Nab2-C_{5-7}→A protein for poly(A) RNA.

DISCUSSION

In this study, we define the RNA binding domain within the tandem CCCH zinc fingers of the polyadenosine RNA-binding protein Nab2. We show through a combination of genetic and biochemical methods that the Nab2 domain containing zinc fingers 5–7 mediates specific high affinity binding to polyadenosine RNA. Amino acid substitutions within the polyadenosine RNA binding domain of Nab2 that disrupt Nab2 binding to poly(A) RNA *in vitro* also impair Nab2 function *in vivo* and result in aberrant control of poly(A) tail length. Interestingly, cells that express these variants of Nab2 show no nuclear accumulation of poly(A) RNA. These findings provide evidence that Nab2 associates with RNA to control poly(A) tail length but that high affinity Nab2 binding to RNA is not required for efficient export of bulk poly(A) RNA from the nucleus.

A close inspection of the Nab2 amino acid sequence reveals seven zinc fingers that are arranged in three clusters consisting of two (ZnF 1–2 and ZnF 3–4) or three (ZnF 5–7) zinc fingers (diagrammed in Fig. 1). The zinc fingers within each cluster are arranged in close proximity to one another, suggesting that they might function as independently folding domains. Consistent with this idea, we identified a self-folding, trypsin-resistant domain consisting of zinc fingers 5–7 that binds with high affinity to polyadenosine RNA. It is tempting to postulate that zinc fingers 5–7 may interact with one another to constitute a specific polyadenosine RNA-binding module.

Although Nab2 zinc fingers 5–7 appear to play a principal role in high affinity binding to polyadenosine RNA, Nab2-ΔZnF 5–7 retains some ability to bind RNA. The weak binding of Nab2-ΔZnF 5–7 to polyadenosine RNA could be mediated by either zinc fingers 1–4 or the RGG domain of Nab2. Importantly, only the third zinc finger cluster (containing ZnF 5–7) contains three zinc fingers, while the other two clusters contain only two zinc fingers. Thus, three consecutive zinc fingers within close proximity to one another may be required for high affinity binding to polyadenosine RNA. In addition to zinc fingers, Nab2 also contains an arginine-glycine-glycine (RGG) repeat-containing domain, a motif that has been characterized as a nucleic acid interaction motif in other proteins (37) and could also mediate weak binding between Nab2-ΔZnF 5–7 and nucleic acids. Although these weak interactions could promote binding of Nab2 to specific mRNA transcripts via interactions between ZnF 1–4 or the RGG domain and sequences within the 3′-UTR of select transcripts, recent evidence suggests that Nab2 is associated with the majority of yeast transcripts (38) consistent with binding to the poly(A) tail of a large number of transcripts.

Importantly, we present evidence that cysteine to alanine amino acid substitutions in zinc fingers 5–7 disrupt polyadenosine RNA binding and also cause defects in poly(A) tail length but do not cause nuclear accumulation of poly(A) RNA, suggesting that Nab2 plays a critical role in the control of poly(A) tail length and that RNA binding is not required for efficient export of RNA from the nucleus. In support of this idea, aromatic residues within zinc fingers 5–7 are also critical for the interaction between Nab2 and polyadenosine RNA. In particular, phenylalanine 450 (Phe-450) within zinc finger 6 appears critical for the interaction between Nab2 and polyadenosine RNA. Substitution of alanine at position 450 not only disrupts RNA binding but also leads to longer poly(A) tails, providing a direct correlation between poly(A) tail length and RNA binding affinity. Although this Phe to Ala substitution is less likely than changes to the structural Cys residues to alter the overall conformation of this domain, our results do suggest that zinc finger 6 may be particularly critical for binding to polyadenosine RNA.

Our finding that RNA binding by Nab2 is critical for proper control of poly(A) tail length is consistent with several previous observations linking Nab2 directly to control of poly(A) tail length (7, 9, 10). Although previous studies have demonstrated that Nab2 controls poly(A) tail length *in vitro* (7, 9) and *in vivo* (7, 10), the RNA binding ability of Nab2 mutants, which show longer poly(A) tails, has not been investigated. For example, cells expressing a Nab2 mutant in which part of the sixth and the entire seventh zinc finger were deleted also caused longer poly(A) tails *in vivo* (7) and *in vitro* (9). Cells expressing this mutant, Nab2-21, also showed a cold-sensitive growth phenotype, similar to Nab2-C_{5-7}→A and Nab2-Y428A,F450A,F471A, but no detailed analyses of changes in RNA binding affinity were performed for the Nab2-21 protein. We present data here that strongly link the RNA binding affinity of zinc fingers 5–7 with poly(A) tail length.

In contrast to the RNA-binding mutants, deletion of the N terminus of Nab2, which targets the protein to the nuclear pore complex (14, 39), causes both nuclear accumulation of poly(A) RNA and extended poly(A) tails (10, 12). Recent evidence suggests that Dbp5 remodels ribonucleoprotein complexes as they exit the nucleus, removing key nuclear factors, including Nab2 (25) and Mex67 (40). According to this model, failure to remove these proteins from the RNA would result in a "back-up" of the assembly line and accumulation of poly(A) RNA in the nucleus. Therefore, mutant proteins that cannot be removed by Dbp5 may be deleterious to the cell. Hence, we propose that mutant versions of Nab2, such as ΔN-Nab2, that cause defects in both poly(A) tail length and poly(A) RNA export from the nucleus may be more difficult to remove from polyadenosine RNA than wild-type Nab2, resulting in a back-up of the RNA assembly line and accumulation of poly(A) RNA in the nucleus. In support of this hypothesis, the ΔN-Nab2 protein is UV cross-linked *in vivo* to poly(A) RNA transcripts at higher levels than wild-type Nab2, and overexpression of ΔN-Nab2 impairs cell growth (12).

A primary requirement for Nab2 binding to RNA for proper mRNA 3′-end processing and not for mRNA export, although somewhat surprising, may be consistent with evidence obtained in other model organisms. A recent genome-wide study investigating the components required for proper export of poly(A) RNA in *Drosophila melanogaster* S2 cells suggests that the putative *D. melanogaster* Nab2 orthologue, CG5720, is not required for mRNA export (41). In addition, recent work characterizing the putative human Nab2 orthologue, ZC3H14, demonstrates that ZC3H14 co-localizes with the nuclear speckle marker, SC35 (5). Nuclear speckles are thought to house factors for the mRNA assembly line as they contain many splicing factors as well as transcription-related proteins that play critical roles in RNA metabolism (reviewed in Ref. 42). Hence, localization of ZC3H14 in nuclear speckles strongly suggests a role in mRNA processing. Overall, the evidence presented here supports the idea that carefully defining a specific protein function, such as RNA binding, and making mutants to disrupt that function, allows for precise definition of a cellular role of that protein. Analysis of these RNA-binding mutants reveals that the interaction of Nab2 with RNA is required for proper control of polyadenylation. Here, we provide insight into the novel mechanism of polyadenosine RNA recognition by the CCCH zinc fingers of Nab2 and define key aromatic residues as at least one element of this molecular recognition.

Acknowledgments—We thank the Corbett laboratory and Murray Stewart for critical analysis and discussion of the manuscript. We also thank Michael Rosbash for providing pap1-1 and rna15-2 yeast strains and Sean Ryder for critical help in establishing the fluorescence anisotropy assays.

REFERENCES

1. Moore, M. J. (2005) *Science* **309,** 1514–1518
2. Pandit, S., Wang, D., and Fu, X. D. (2008) *Curr. Opin. Cell Biol.* **20,** 260–265
3. Luna, R., Gaillard, H., González-Aguilera, C., and Aguilera, A. (2008) *Chromosoma* **117,** 319–331
4. Buratowski, S., and Moazed, D. (2005) *Nature* **435,** 1174–1175
5. Leung, S. W., Apponi, L. H., Cornejo, O. E., Kitchen, C. M., Valentini, S. R., Pavlath, G. K., Dunham, C. M., and Corbett, A. H. (2009) *Gene* **439,** 71–78
6. Kelly, S. M., Pabit, S. A., Kitchen, C. M., Guo, P., Marfatia, K. A., Murphy, T. J., Corbett, A. H., and Berland, K. M. (2007) *Proc. Natl. Acad. Sci. U.S.A.* **104,** 12306–12311
7. Hector, R. E., Nykamp, K. R., Dheur, S., Anderson, J. T., Non, P. J., Urbinati, C. R., Wilson, S. M., Minvielle-Sebastia, L., and Swanson, M. S. (2002) *EMBO J.* **21,** 1800–1810
8. Mangus, D. A., Evans, M. C., and Jacobson, A. (2003) *Genome Biol.* **4,** 223
9. Viphakone, N., Voisinet-Hakil, F., and Minvielle-Sebastia, L. (2008) *Nucleic Acids Res.* **36,** 2418–2433
10. Chekanova, J. A., and Belostotsky, D. A. (2003) *RNA* **9,** 1476–1490
11. Dheur, S., Nykamp, K. R., Viphakone, N., Swanson, M. S., and Minvielle-Sebastia, L. (2005) *J. Biol. Chem.* **280,** 24532–24538
12. Marfatia, K. A., Crafton, E. B., Green, D. M., and Corbett, A. H. (2003) *J. Biol. Chem.* **278,** 6731–6740
13. Anderson, J. T., Wilson, S. M., Datar, K. V., and Swanson, M. S. (1993) *Mol. Cell. Biol.* **13,** 2730–2741
14. Fasken, M. B., Stewart, M., and Corbett, A. H. (2008) *J. Biol. Chem.* **283,** 27130–27143
15. Vinciguerra, P., Iglesias, N., Camblong, J., Zenklusen, D., and Stutz, F. (2005) *EMBO J.* **24,** 813–823
16. Green, D. M., Johnson, C. P., Hagan, H., and Corbett, A. H. (2003) *Proc. Natl. Acad. Sci. U.S.A.* **100,** 1010–1015
17. Fasken, M. B., and Corbett, A. H. (2009) *RNA Biol.* **6,** 237–241
18. Hammell, C. M., Gross, S., Zenklusen, D., Heath, C. V., Stutz, F., Moore, C., and Cole, C. N. (2002) *Mol. Cell. Biol.* **22,** 6441–6457
19. Hilleren, P., and Parker, R. (2001) *RNA* **7,** 753–764
20. Lunde, B. M., Moore, C., and Varani, G. (2007) *Nat. Rev. Mol. Cell Biol.* **8,** 479–490
21. Sambrook, J., Fritsch, E. F., and Maniatis, T. (1989) *Molecular Cloning: A Laboratory Manual*, 2nd Ed, Cold Spring Harbor Laboratory Press, Cold Spring Harbor, NY
22. Adams, A., Gottschling, D. E., Kaiser, C. A., and Stearns, T. (1997) *Methods in Yeast Genetics: A Cold Spring Harbor Laboratory Course Manual*, Cold Spring Harbor Laboratory Press, Cold Spring Harbor, NY
23. Wach, A., Brachat, A., Pöhlmann, R., and Philippsen, P. (1994) *Yeast* **10,** 1793–1808
24. Boeke, J. D., Trueheart, J., Natsoulis, G., and Fink, G. R. (1987) *Methods Enzymol.* **154,** 164–175
25. Tran, E. J., Zhou, Y., Corbett, A. H., and Wente, S. R. (2007) *Mol. Cell* **28,** 850–859
26. Pagano, J. M., Farley, B. M., McCoig, L. M., and Ryder, S. P. (2007) *J. Biol. Chem.* **282,** 8883–8894
27. Minvielle-Sebastia, L., Winsor, B., Bonneaud, N., and Lacroute, F. (1991) *Mol. Cell. Biol.* **11,** 3075–3087
28. Apponi, L. H., Leung, S. W., Williams, K. R., Valentini, S. R., Corbett, A. H.,

and Pavlath, G. K. (2010) *Hum. Mol. Genet.* **19,** 1058–1065
29. Wong, D. H., Corbett, A. H., Kent, H. M., Stewart, M., and Silver, P. A. (1997) *Mol. Cell. Biol.* **17,** 3755–3767
30. Tseng, S. S., Weaver, P. L., Liu, Y., Hitomi, M., Tartakoff, A. M., and Chang, T. H. (1998) *EMBO J.* **17,** 2651–2662
31. Schmitt, C., von Kobbe, C., Bachi, A., Panté, N., Rodrigues, J. P., Boscheron, C., Rigaut, G., Wilm, M., Séraphin, B., Carmo-Fonseca, M., and Izaurralde, E. (1999) *EMBO J.* **18,** 4332–4347
32. Strahm, Y., Fahrenkrog, B., Zenklusen, D., Rychner, E., Kantor, J., Rosbach, M., and Stutz, F. (1999) *EMBO J.* **18,** 5761–5777
33. Snay-Hodge, C. A., Colot, H. V., Goldstein, A. L., and Cole, C. N. (1998) *EMBO J.* **17,** 2663–2676
34. Hall, T. M. (2005) *Curr. Opin. Struct. Biol.* **15,** 367–373
35. Brayer, K. J., Kulshreshtha, S., and Segal, D. J. (2008) *Cell Biochem. Biophys.* **51,** 9–19
36. Patel, D., and Butler, J. S. (1992) *Mol. Cell. Biol.* **12,** 3297–3304
37. Zanotti, K. J., Lackey, P. E., Evans, G. L., and Mihailescu, M. R. (2006) *Biochemistry* **45,** 8319–8330
38. Batisse, J., Batisse, C., Budd, A., Böttcher, B., and Hurt, E. (2009) *J. Biol. Chem.* **284,** 34911–34917
39. Grant, R. P., Marshall, N. J., Yang, J. C., Fasken, M. B., Kelly, S. M., Harreman, M. T., Neuhaus, D., Corbett, A. H., and Stewart, M. (2008) *J. Mol. Biol.* **376,** 1048–1059
40. Lund, M. K., and Guthrie, C. (2005) *Mol. Cell* **20,** 645–651
41. Farny, N. G., Hurt, J. A., and Silver, P. A. (2008) *Genes Dev.* **22,** 66–78
42. Handwerger, K. E., and Gall, J. G. (2006) *Trends Cell Biol.* **16,** 19–26
43. Sikorski, R. S., and Hieter, P. (1989) *Genetics* **122,** 19–27
44. Matsuura, Y., and Stewart, M. (2004) *Nature* **432,** 872–877

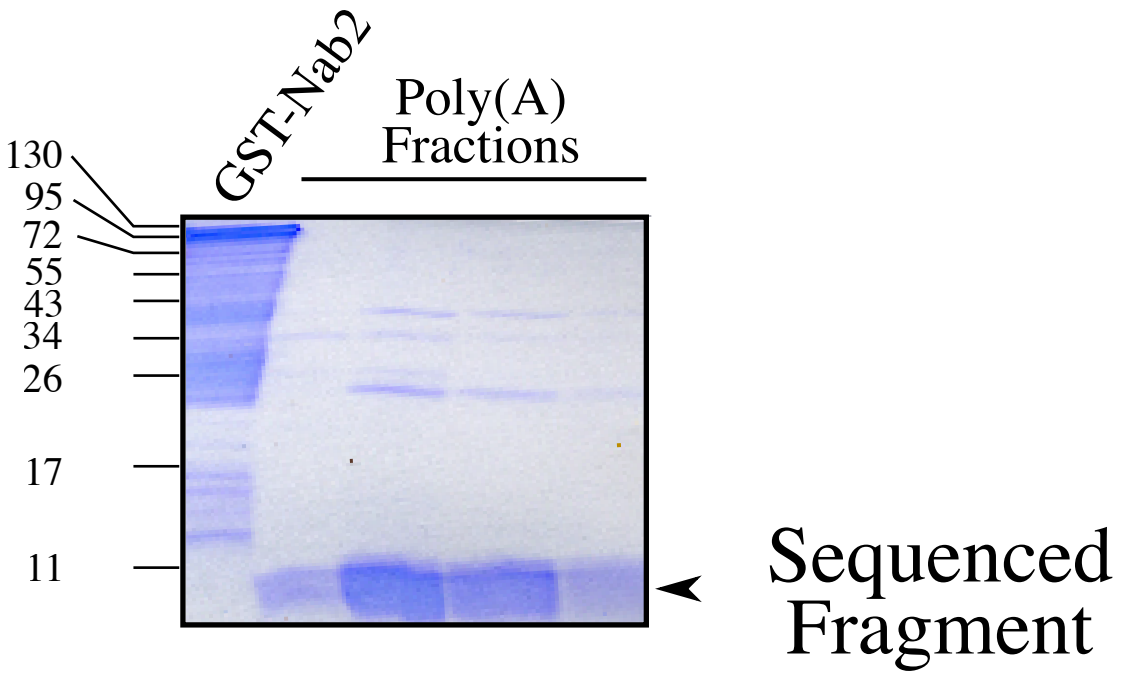

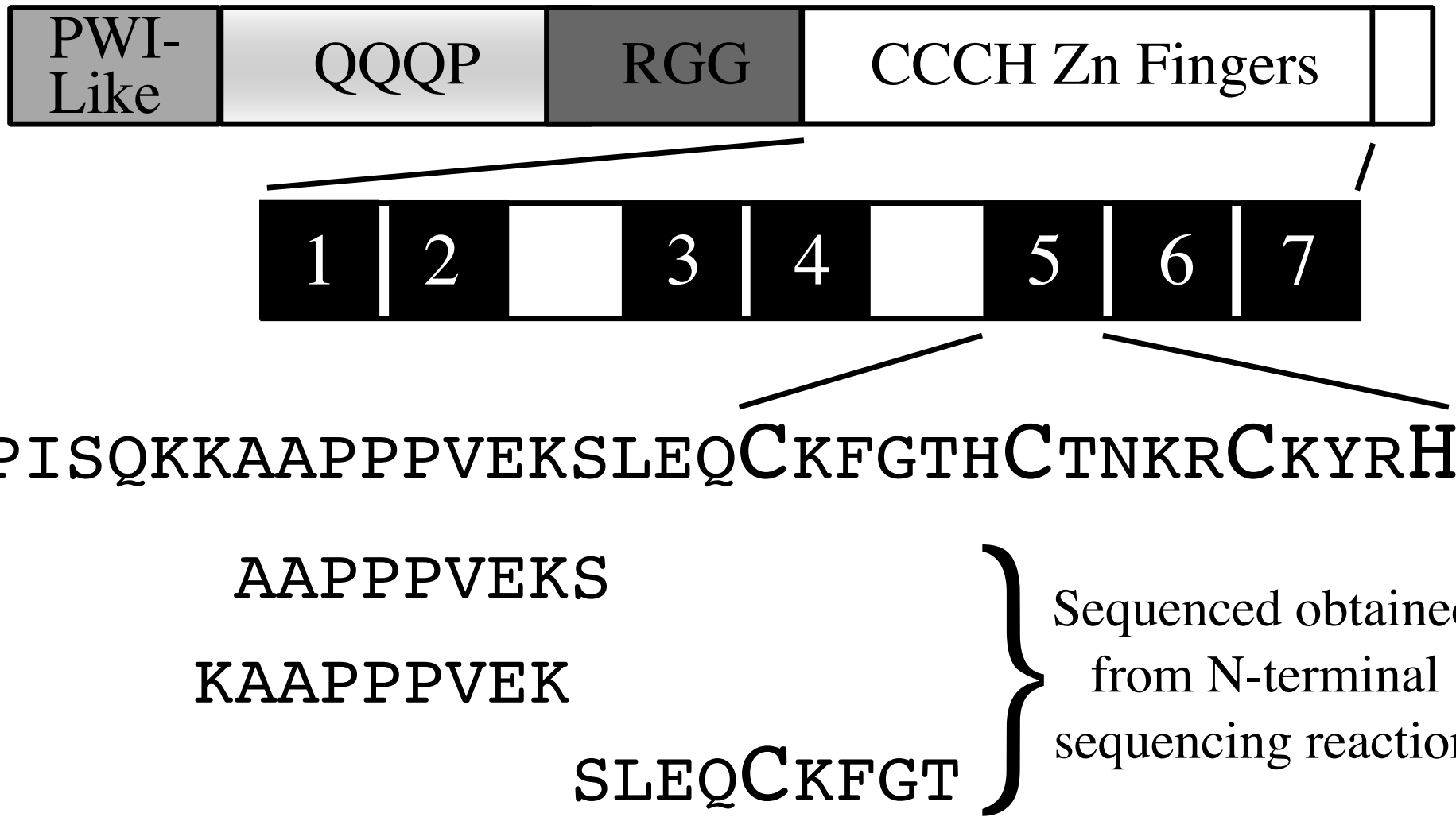

Kelly et al. Supp. Data Figure 1

A.

ZnF1	258	KEGRCRLFPHCPLGRS-CPHAHPTKV	282
ZnF2	279	PTKVCNEYPNCPKPPGTCEFLHPNED	304
ZnF3	336	GIVLCKFGALCSNPS--CPFGHPTPA	359
ZnF4	367	DLMWCDKNLTCDNPE--CRKAHSSLS	390
ZnF5	411	SLEQCKFGTHCTNKR--CKYRHARSH	434
ZnF6	433	SHIMCREGANCTRID--CLFGHPINE	456
ZnF7	454	INEDCRFGVNCKNIY--CLFRHPPGR	477

B.

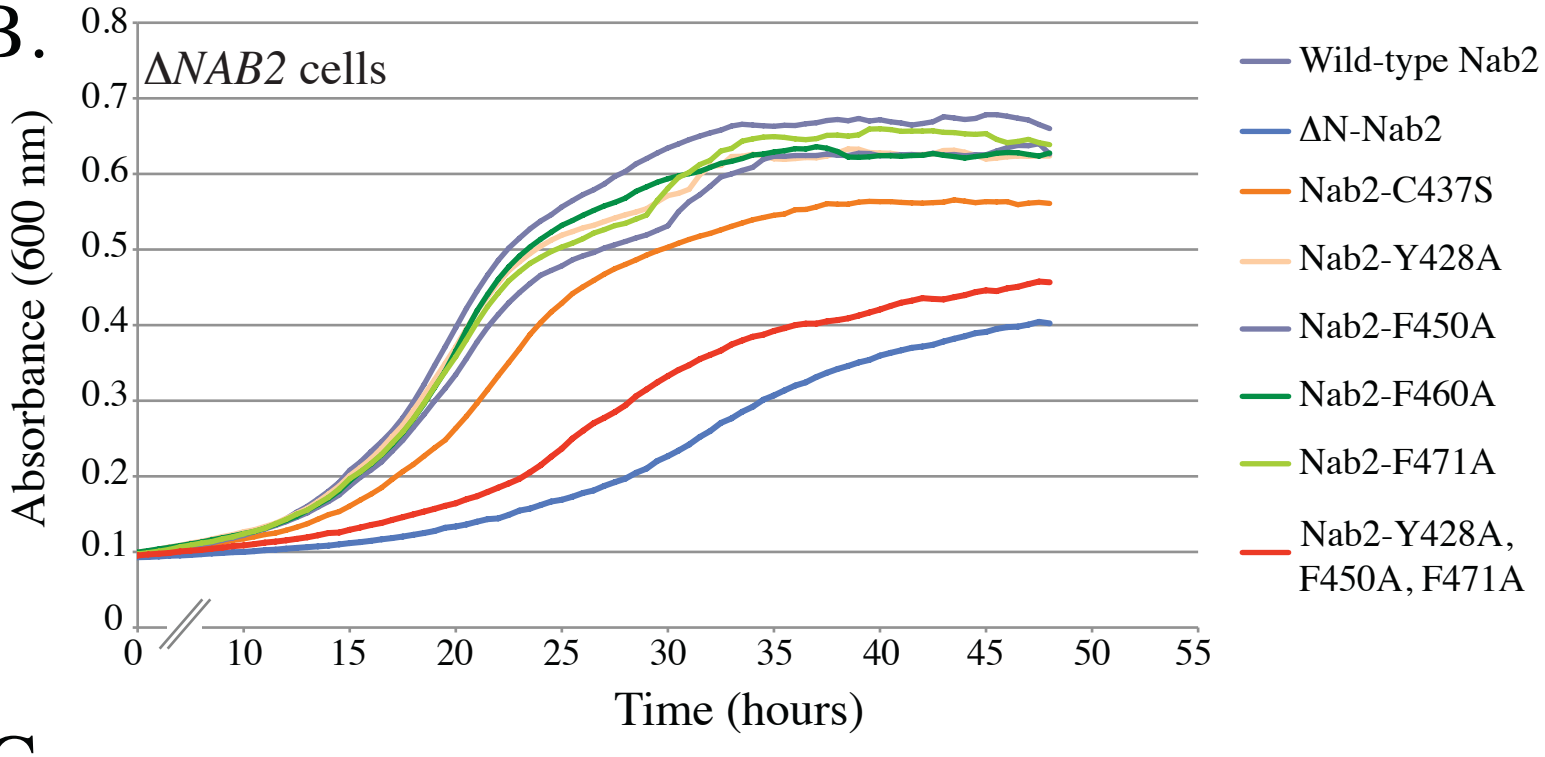

C.

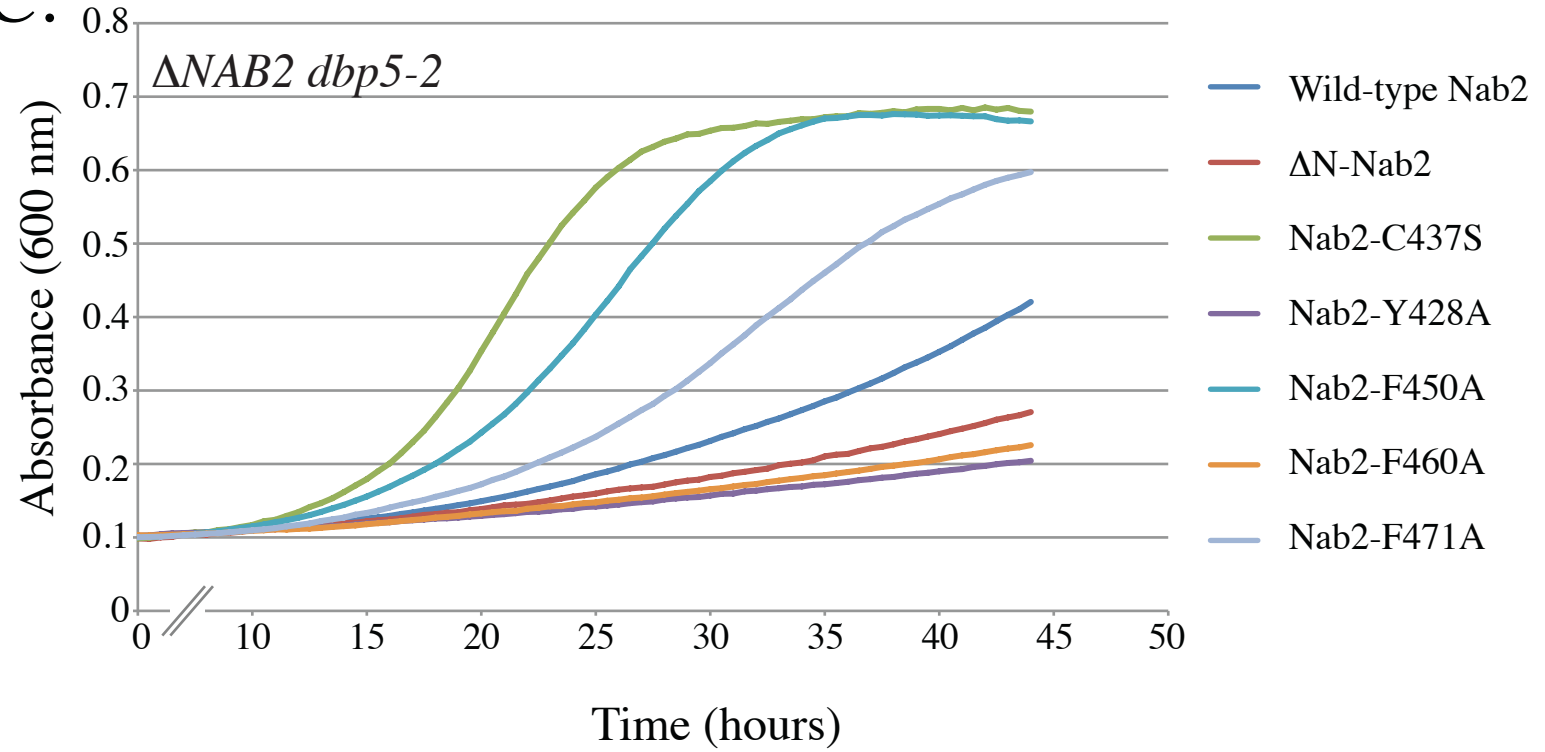

Kelly et al. Supp. Figure 2

Recognition of Polyadenosine RNA by the Zinc Finger Domain of Nuclear Poly(A) RNA-binding Protein 2 (Nab2) Is Required for Correct mRNA 3′-End Formation*

Seth M. Kelly, Sara W. Leung, Luciano H. Apponi, Anna M. Bramley, Elizabeth J. Tran, Julia A. Chekanova, Susan R. Wente and Anita H. Corbett

J. Biol. Chem. 2010, 285:26022-26032.
doi: 10.1074/jbc.M110.141127 originally published online June 16, 2010
